DR UPPULURI V. MALLAVADHANI (Orcid ID : 0000-0003-1806-9164)

Article type : Research Article

Novel Menadione Hybrids: Synthesis, anticancer activity and cell based studies

Chakka Vara Prasad [1], Vadithe Lakshma Nayak [2], Sistla Ramakrishna [2], Uppuluri Venkata Mallavadhani [1,*]

[1] Natural Products Chemistry Division, CSIR-Indian Institute of Chemical Technology, Hyderabad, 500007, India

[2] Department of Medicinal Chemistry & Pharmacology, CSIR-Indian Institute of Chemical Technology, Hyderabad, 500007, India

* Corresponding author: Natural Products Chemistry Division, CSIR-Indian Institute of Chemical Technology, Hyderabad 500007, India.

E- Mail address: uvmavadani@yahoo.com (U. V. Mallavadhani)

Keywords**:** *1,4-Naphthoquinone, Menadione, 1,2,3-Triazole, Cytotoxicity, Apoptosis, Cell cycle arrest.*

ABSTRACT

A series of novel menadione based triazole hybrids were designed and synthesized by employing copper catalyzed azide-alkyne cycloaddition (CuAAC). All the synthesized hybrids were characterized by their spectral data (^{1}H NMR, ^{13}C NMR, IR and HRMS). The synthesized compounds were evaluated for their anticancer activity against five selected cancer cell lines including lung (A549), prostate (DU-145), cervical (Hela),

This article has been accepted for publication and undergone full peer review but has not been through the copyediting, typesetting, pagination and proofreading process, which may lead to differences between this version and the Version of Record. Please cite this article as doi: 10.1111/cbdd.13073

breast (MCF-7) and mouse melanoma (B-16) by using MTT assay. The screening results showed that majority of the synthesized compounds displayed significant anticancer activity. Among the tested compounds, the triazoles **5** and **6** exhibited potent activity against all cell lines. In particular, compound **6** showed higher potency than the standard tamoxifen and parent menadione against MCF-7 cell line. Flow cytometric analysis revealed that compound **6** arrested cell cycle at G0/G1 phase and induced apoptotic cell death which was further confirmed by Hoechst staining, measurement of mitochondrial membrane potential ($\Delta\Psi$m) and Annexin V-FITC assay. Thus, compound **6** can be considered as lead molecule for further development as potent anticancer therapeutic agent.

Introduction

Quinones are widely distributed in nature as secondary metabolites. Both natural quinones and their synthetic analogues possess broad spectrum of biological activities, including antifungal, antibacterial, antimalarial, antiviral and anticancer activity [1–3]. Moreover, the quinone scaffold is present in many clinically useful cancer drugs such as daunorubicin, doxorubicin, saintopin, mitomycin and mitoxantrone (**Figure 1**). The most important chemical class in the quinone family is the 1,4-naphthoquinones. Recently naturally occurring 1,4-naphthoquinones such as menadione (vitamin K3), juglone and plumbagin have grabbed attention for their significant anticancer activity against various cancer cell lines as well as *in vivo* in animal models [4–6]. Particularly, menadione has been reported to exhibit *in vitro* anticancer activity against mammary, breast, hepatic, blood, bladder and oral cancer cell lines [7, 8]. Menadione was effective even against multi-drug-resistant leukemia cell lines and parental leukemia cell lines [9, 10]. The main mechanism of the cytotoxicity of menadione in cancer cells involves the oxidative stress via redox cycling of quinone to produce reactive oxygen species (ROS), which leads to

DNA damage and cell death [11]. A phase I clinical study showed that menadione is reasonably well tolerated and menadione showed synergistic cytotoxicity effect with other anticancer drugs such as 5-FU, bleomycin, mitomycin C and vitamin C [12]. Due to its remarkable bioactivities, much more effort has been devoted in synthesizing novel analogues of menadione with newer and enhanced cytotoxic activities.

The triazole ring system is a very well-recognized pharmacophore. This five-membered heterocycle is a prominent among U.S FDA approved pharmaceuticals, possesses aromaticity and is an electron rich system [13]. This unique structure endows triazole derivatives to readily bind to a variety of enzymes and receptors in biological system via non-covalent interactions, thus displaying a large array of biological activities. In particular, 1,2,3-triazoles have received much attention in drug discovery due to their wide range of biological activities such as anticancer, anti-HIV, anti-influenza, antimalarial, antituberculosis, anti-inflammatory, antibacterial and antifungal [14, 15]. In addition, several drugs either in the market or in the final stage of clinical trials contain 1,2,3-triazole group. Some of the important 1,2,3-triazole based therapeutic agents are tazobactam (antibiotic), radezolid (antibiotic), rufinamide (anticonvulsant), carboxyamidotriazole orotate (known as CTO, anticancer), tert-butyldimethylsilylspiroaminooxathioledioxide (known as TSAO, HIV reverse transcriptase inhibitor) (**Figure 1**). Considering the fact that combination of two pharmacophores in a single molecule is a versatile tool for drug discovery developments, we aimed to synthesize a series of novel menadione based 1,2,3-triazole hybrids.

Methods and Materials

Chemistry

Solvents were distilled before use. Reagents were procured from commercial sources (Sigma-Aldrich, Alfa Aesar) and used without further purification. All reactions were monitored by pre-coated silica gel 60 F_{254} glass TLC plates (Merck) with UV irradiation at 254 nm or exposure to iodine vapours for visualization. Column chromatography was carried on silica gel (60-120 mesh). Melting points were determined on a Stuart SMP3 digital melting point apparatus and are uncorrected. IR spectra were recorded on Nicolet Nexus 670 spectrophotometer using KBr pellets. ^{1}H and ^{13}C NMR spectra were recorded on Bruker 400 MHz and 500 MHz in $CDCl_3$ with TMS as internal standard. Chemical shifts were expressed as δ values in parts per million (ppm) and coupling constants (*J*) in Hertz (Hz). HRMS spectra were recorded on Agilent-ESI QTOF and JEOL mass spectrometers.

General procedure for the synthesis of azidoaminoalkanes (**2**)

Method A (for compounds **2a-b)**:

To a solution of n-bromoalkylammonium bromide (9.7 mmol) in water (20 mL) was added sodium azide (29.2 mmol) and the mixture was heated at 80 ^{o}C for 15 h. After removing about 10 mL of water in vacuum, the resulting solution was cooled in an ice bath and diethyl ether (50 mL) and KOH pellets (4 g) were added, keeping the temperature below 10 ^{o}C. The organic layer was separated and the aqueous layer was further extracted with diethyl ether (2 x 50 mL). The combined organic layers were dried

over K_2CO_3 and concentrated to give the corresponding desired products **2a** and **2b** in 78 % and 82% yields respectively.

Method B (for compounds **2c-d**):

Step 1

To a solution of dibromoalkane compound (9.2 mmol) in DMF (10 mL) was added an aqueous solution of sodium azide (19.3 mmol in 5 mL water). The mixture was stirred and heated at 80 ^oC for 20 h, and then the medium was washed with brine (20 mL) and extracted with hexane (3 x 30 mL). The combined organic layer was dried over Na_2SO_4 and concentrated to give diazidoalkanes as liquids, which were used directly in the next step.

Step 2

To a solution of diazidoalkane (9.2 mmol) in Et_2O (6 mL) : EtOAc (6 mL) and 5 % HCl (10 mL) was added triphenylphosphine (9 mmol) in small portions for 1 h at 0 ^oC and then the mixture was stirred for 24 h at room temperature. The organic layer was discarded and the aqueous layer was washed twice with DCM (15 mL). The resulting aqueous layer was carefully basified with NaOH and then extracted with DCM (3 x 15 mL). The combined extracts were dried over Na_2SO_4 and concentrated to yield azidoaminoalkanes, which were used directly to synthesis Michael adducts.

General procedure for the synthesis of Michael adducts **3a-d**

Menadione **1** (1 g, 5.8 mmol) was added to a solution of azidoamino alkane **2** (8.7 mmol) in 6 mL DCM. The resulting red colour solution was stirred at room temperature

and progress of reaction was monitored by TLC. After 48 h, reaction was completed and reaction mixture was concentrated under vacuum and purified by silica gel column chromatography with hexane: ethyl acetate (94:6) as eluent to afford the title compounds **3a-d**.

2-((2-azidoethyl)amino)-3-methylnaphthalene-1,4-dione (**3a**)

Yield 19 %; dark red solid; mp 80-82 ^{o}C; R_f 0.37 (hexane/ethyl acetate 4:1); IR (KBr, cm^{-1}): 3314, 2928, 2103, 1672, 1600, 1567, 1514, 1461; ^{1}H NMR (500 MHz, $CDCl_3$): δ 2.20 (3H, s), 3.56 (2H, t, *J* = 5.4 Hz), 3.73 (2H, t, *J* = 5.4 Hz), 5.75 (1H, bs), 7.60 (1H, td, *J* = 7.4, 1.3 Hz), 7.68 (1H, td, *J* = 7.4, 1.3 Hz), 8.01 (1H, dd, *J* = 7.6, 1.0 Hz), 8.08 (1H, dd, *J* = 7.6, 1.0 Hz); ^{13}C NMR (125 MHz, $CDCl_3$): δ 11.16, 44.24, 51.53, 113.98, 126.00, 126.14, 130.26, 132.03, 133.04, 134.24, 145.72, 182.10, 183.49; HRMS (ESI): m/z calcd for $C_{13}H_{12}N_4O_2Na$ $(M+Na)^+$ 279.0852 found 279.0839.

2-((3-azidopropyl)amino)-3-methylnaphthalene-1,4-dione (**3b**)

Yield 17 %; dark red solid; mp 67-69 ^{o}C; R_f 0.42 (hexane/ethyl acetate 4:1); IR (KBr, cm^{-1}): 3339, 2924, 2857, 2099, 1665, 1599, 1565, 1523, 1466; ^{1}H NMR (400 MHz, $CDCl_3$): δ 1.90 (2H, quint, *J* = 6.3 Hz) 2.23 (3H, s), 3.45 (2H, t, *J* = 6.3 Hz), 3.66 (2H, t, *J* = 6.8 Hz), 5.70 (1H, bs), 7.58 (1H, td, *J* = 7.5, 1.3 Hz), 7.68 (1H, td, *J* = 7.5, 1.3 Hz), 7.99 (1H, dd, *J* = 7.5, 1.1 Hz), 8.08 (1H, dd, *J* = 7.5, 1.1 Hz); ^{13}C NMR (125 MHz, $CDCl_3$): δ 11.11, 30.00, 42.67, 48.75, 112.93, 125.93, 126.14, 130.19, 131.86, 133.25, 134.26, 145.84, 182.30, 183.47; HRMS (ESI): m/z calcd for $C_{14}H_{14}N_4O_2Na$ $(M+Na)^+$ 293.1009 found 293.1013.

2-((4-azidobutyl)amino)-3-methylnaphthalene-1,4-dione (**3c**)

Yield 15 %; dark red solid; mp 72-74 ^{o}C; R_f 0.47 (hexane/ethyl acetate 4:1); IR (KBr, cm^{-1}): 3278, 2923, 2854, 2093, 1670, 1605, 1568, 1507, 1453; ^{1}H NMR (400 MHz, $CDCl_3$): δ 1.71 (4H, m), 2.23 (3H, s), 3.35 (2H, t, *J* = 6.2 Hz), 3.58 (2H, q, *J* = 6.2 Hz), 5.68 (1H, bs), 7.57 (1H, td, *J* = 7.5, 1.3 Hz), 7.67 (1H, td, *J* = 7.5, 1.3 Hz), 7.99 (1H, dd, *J* = 7.5, 1.1 Hz), 8.08 (1H, dd, *J* = 7.5, 1.1 Hz); ^{13}C NMR (125 MHz, $CDCl_3$): δ 11.17, 26.08, 28.16, 44.88, 50.98, 112.52, 125.94, 126.14, 130.20, 131.83, 133.34, 134.27, 145.92, 182.38, 183.51; HRMS (ESI): m/z calcd for $C_{15}H_{17}N_4O_2$ $(M+H)^+$ 285.1346 found 285.1343.

2-((5-azidopentyl)amino)-3-methylnaphthalene-1,4-dione (**3d**)

Yield 14 %; dark red solid; mp 56-58 ^{o}C; R_f 0.54 (hexane/ethyl acetate 4:1); IR (KBr, cm^{-1}): 3290, 2925, 2858, 2098, 1669, 1603, 1567, 1507, 1453; ^{1}H NMR (500 MHz, $CDCl_3$): δ 1.48 (2H, m), 1.66 (4H, m, *J* = 7.0, 6.8 Hz), 2.23 (3H, s), 3.30 (2H, t, *J* = 6.8 Hz), 3.56 (2H, t, *J* = 7.0 Hz), 7.57 (1H, td, *J* = 7.4, 1.2 Hz), 7.67 (1H, td, *J* = 7.4, 1.2 Hz), 7.99 (1H, dd, *J* = 7.6, 1.0 Hz), 8.08 (1H, dd, *J* = 7.6, 1.0 Hz); ^{13}C NMR (125 MHz, $CDCl_3$): δ 11.14, 23.85, 28.50, 30.43, 45.18, 51.12, 112.21, 125.88, 126.09, 130.17, 131.74, 133.36, 134.23, 145.94, 182.37, 183.45; HRMS (ESI): m/z calcd for $C_{16}H_{19}N_4O_2$ $(M+H)^+$ 299.1502 found 299.1500.

General procedure for the synthesis of menadione-triazole hybrids (4-18)

To a stirred solution of compound **3a** (0.1 g, 0.39 mmol) and appropriate alkyne (0.39 mmol) in THF:H_2O (4:4 mL), $CuSO_4 \cdot 5H_2O$ (0.08 mmol) and sodium ascorbate (0.15 mmol) were added. The reaction mixture was stirred at room temperature for 12 h. After completion of the reaction (monitored by TLC), the reaction mixture was diluted with water and extracted with $CHCl_3$ (3 x 15 mL). The combined organic layer was dried over Na_2SO_4 and concentrated under vacuum. The resulting residue was purified by silica gel column chromatography using a gradient mixture of hexane/ethyl acetate with increasing polarity up to 100% ethyl acetate as an eluent to afford the desired product.

2-methyl-3-((2-(4-phenyl-1H-1,2,3-triazol-1-yl)ethyl)amino)naphthalene-1,4-dione (**4**)

Orange solid; R_f 0.38 (hexane/ethyl acetate 1:1); IR (KBr, cm^{-1}): 3280, 2923, 2853, 1671, 1607, 1568, 1526, 1465; ^{1}H NMR (400 MHz, $CDCl_3$): δ 2.15 (3H, s), 4.14 (2H, t), 4.63 (2H, t, *J* = 5.6 Hz), 5.61 (1H, s, bs), 7.32 (1H, t, *J* = 7.2 Hz), 7.40 (2H, t, *J* = 7.2 Hz), 7.57 (1H, t, *J* = 7.3 Hz), 7.66 (1H, t, *J* = 7.3 Hz), 7.76-7.78 (3H, m) 7.97 (1H, d, *J* = 7.5 Hz), 8.04 (1H, d, *J* = 7.5 Hz); ^{13}C NMR (125 MHz, $CDCl_3$): δ 10.91, 45.06, 50.78, 115.30, 120.31, 125.70, 126.01, 126.16, 128.28, 128.81, 130.15, 130.39, 132.15, 132.84, 134.25, 145.63, 148.08, 182.25, 183.31; HRMS (ESI): m/z calcd for $C_{21}H_{19}N_4O_2$ $(M+H)^+$ 359.1502 found 359.1494.

2-methyl-3-((2-(4-(p-tolyl)-1H-1,2,3-triazol-1-yl)ethyl)amino)naphthalene-1,4-dione (**5**)

Dark red solid; R_f 0.32 (hexane/ethyl acetate 1:1); IR (KBr, cm^{-1}): 3330, 3106, 2922, 1667, 1602, 1563, 1500, 1459; ^1H NMR (500 MHz, $CDCl_3$): δ 2.14 (3H, s), 2.37 (3H, s), 4.13 (2H, t, *J* = 5.6 Hz), 4.62 (2H, t, *J* = 5.6 Hz), 5.61 (1H, bs), 7.20 (2H, d, *J* = 7.9 Hz), 7.57 (1H, t, *J* = 7.4 Hz), 7.65-7.68 (3H, m), 7.73 (1H, s), 7.97 (1H, d, *J* = 7.6 Hz), 8.04 (1H, d, *J* = 7.6 Hz); ^{13}C NMR (100 MHz, $CDCl_3$): δ 10.88, 21.23, 45.04, 50.70, 115.12, 119.99, 125.59, 125.98, 126.11, 127.34, 129.46, 130.37, 132.09, 132.82, 134.19, 138.12, 145.63, 148.12, 182.19, 183.26; HRMS (ESI): m/z calcd for $C_{22}H_{21}N_4O_2$ $(M+H)^+$ 373.1659 found 373.1659.

2-((2-(4-(4-ethylphenyl)-1H-1,2,3-triazol-1-yl)ethyl)amino)-3-methylnaphthalene-1,4-dione (**6**)

Yellow solid; R_f 0.33 (hexane/ethyl acetate 1:1); IR (KBr, cm^{-1}): 3328, 3103, 2959, 2925, 1657, 1634, 1613, 1587,1492, 1461; ^1H NMR (500 MHz, $CDCl_3$): δ 1.25 (3H, t, *J* = 7.6 Hz), 2.14 (3H, s), 2.66 (2H, q, *J* = 7.6 Hz), 4.13 (2H, t, *J* = 5.4 Hz), 4.62 (2H, t, *J* = 5.4 Hz), 5.61 (1H, bs), 7.23 (2H, d, *J* = 8.2 Hz), 7.57 (1H, td, *J* = 7.6, 1.2 Hz), 7.66 (1H, td, *J* = 7.6, 1.2 Hz), 7.69 (2H, d, *J* = 8.2 Hz), 7.73 (1H, s), 7.97 (1H, dd, *J* = 7.6, 1.2 Hz), 8.04 (1H, dd, *J* = 7.6, 1.2 Hz), ^{13}C NMR (125 MHz, $CDCl_3$): δ 10.90, 15.47, 28.63, 45.06, 50.73, 115.26, 119.97, 125.70, 126.02, 126.16, 127.58, 128.30, 130.40, 132.13, 132.84, 134.23, 144.52, 145.64, 148.18, 182.24, 183.30; HRMS (ESI): m/z calcd for $C_{23}H_{23}N_4O_2$ $(M+H)^+$ 387.1815 found 387.1812.

2-methyl-3-((2-(4-(4-propylphenyl)-1H-1,2,3-triazol-1-yl)ethyl)amino)naphthalene-1,4-dione (**7**)

Red solid; R_f 0.36 (hexane/ethyl acetate 1:1); IR (KBr, cm^{-1}): 3327, 3107, 2923, 2859, 1669, 1600, 1565, 1499, 1457; ^{1}H NMR (400 MHz, $CDCl_3$): δ 0.95 (3H, t, *J* = 7.3 Hz), 1.61-1.70 (2H, m, *J* = 7.3 Hz), 2.14 (3H, s), 2.60 (2H, t, *J* = 7.3 Hz), 4.13 (2H, t, *J* = 5.6 Hz), 4.62 (2H, t, *J* = 5.6 Hz), 5.61 (1H, bs), 7.21 (2H, d, *J* = 8.1 Hz), 7.57 (1H, td, *J* = 7.5, 1.3 Hz), 7.64-7.69 (3H, m, *J* = 7.5 Hz), 7.73 (1H, s), 7.97 (1H, dd, *J* = 7.5, 1.1 Hz), 8.04 (1H, dd, *J* = 7.5, 1.1 Hz); ^{13}C NMR (100 MHz, $CDCl_3$): δ 10.89, 13.75, 24.42, 37.76, 45.05, 50.70, 115.14, 120.00, 125.58, 125.99, 126.11,127.58, 128.89, 130.38, 132.09, 132.82, 134.19, 142.94, 145.64, 148.16, 182.21, 183.26; HRMS (ESI): m/z calcd for $C_{24}H_{25}N_4O_2$ $(M+H)^+$ 401.1972 found 401.1974.

2-((2-(4-(4-(tert-butyl)phenyl)-1H-1,2,3-triazol-1-yl)ethyl)amino)-3-methylnaphthalene-1,4-dione (**8**)

Dark red solid; R_f 0.36 (hexane/ethyl acetate 1:1); IR (KBr, cm^{-1}): 3334, 3152, 2957, 1663, 1601, 1566, 1514, 1468; ^{1}H NMR (500 MHz, $CDCl_3$): δ 1.34 (9H, s), 2.14 (3H, s), 4.14 (2H, t, *J* = 5.6 Hz), 4.63 (2H, t, *J* = 5.6 Hz), 5.58 (1H, bs), 7.42 (2H, d, *J* = 8.5 Hz), 7.57 (1H, td, *J* = 7.6, 1.3 Hz), 7.66 (1H, td, *J* = 7.6, 1.3 Hz) 7.70 (2H, d, *J* = 8.3 Hz), 7.73 (1H, s), 7.97 (1H, dd, *J* = 7.6, 1.0 Hz), 8.04 (1H, dd, *J* = 7.6, 1.0 Hz); ^{13}C NMR (125 MHz, $CDCl_3$): δ 10.92, 31.25, 34.65, 45.08, 50.76, 115.36, 120.00, 125.46, 126.04, 126.19, 127.34, 130.43, 132.14, 132.87, 134.24, 145.65, 148.11, 151.42, 182.26, 183.33; HRMS (ESI): m/z calcd for $C_{25}H_{27}N_4O_2$ $(M+H)^+$ 415.2129 found 415.2127.

2-((2-(4-(4-methoxyphenyl)-1H-1,2,3-triazol-1-yl)ethyl)amino)-3-methylnaphthalene-1,4-dione (**9**)

Dark red solid; R_f 0.53 (hexane/ethyl acetate 1:2.3); IR (KBr, cm^{-1}): 3339, 3103, 2923, 1665, 1599, 1563, 1499, 1457; ^1H NMR (400 MHz, $CDCl_3$): δ 2.15 (3H, s), 3.83 (3H, s), 4.13 (2H, t, *J* = 5.6 Hz), 4.62 (2H, t, *J* = 5.6 Hz), 5.62 (1H, bs), 6.93 (2H, d, *J* = 8.6 Hz), 7.57 (1H, t, *J* = 6.8 Hz), 7.64-7.71 (4H, m), 7.97 (1H, d, *J* = 7.5 Hz), 8.04 (1H, d, *J* = 7.5 Hz); ^{13}C NMR (125 MHz, $CDCl_3$): 10.91, 45.06, 50.71, 55.29, 114.21, 115.22, 119.52, 122.86, 126.15, 127.02, 130.40, 132.13, 134.23, 145.65, 147.94, 159.67, 182.24, 183.30; HRMS (ESI): m/z calcd for $C_{22}H_{20}N_4O_3Na$ $(M+Na)^+$ 411.1428 found 411.1437.

2-methyl-3-((2-(4-(4-(trifluoromethoxy)phenyl)-1H-1,2,3-triazol-1-yl)ethyl)amino)naphthalene-1,4-dione (**10**)

Orange solid; R_f 0.64 (hexane/ethyl acetate 1:2.3); IR (KBr, cm^{-1}): 3301, 3118, 2924, 1674, 1608, 1568, 1502; ^1H NMR (400 MHz, $CDCl_3$): δ 2.14 (3H, s), 4.14 (2H, t, *J* = 5.6 Hz), 4.64 (2H, t, *J* = 5.6 Hz), 5.57 (1H, bs), 7.24 (2H, d, *J* = 8.8 Hz), 7.57 (1H, td, *J* = 7.5, 1.3 Hz), 7.65 (1H, td, *J* = 7.5, 1.3 Hz), 7.76 (1H, s), 7.77-7.80 (2H, m, *J* = 8.8 Hz), 7.96 (1H, dd, *J* = 7.5, 0.9 Hz), 8.03 (1H,dd, *J* = 7.5, 0.9 Hz); ^{13}C NMR (100 MHz, $CDCl_3$): 10.97, 45.04, 50.93, 115.54, 119.13, 120.55, 121.32, 125.99, 126.18, 127.06, 128.92, 130.34, 132.18, 132.79, 134.28, 145.61, 146.79, 149.01, 182.27, 183.31; HRMS (ESI): m/z calcd for $C_{22}H_{17}F_3N_4O_3Na$ $(M+Na)^+$ 465.1145 found 465.1163.

2-((2-(4-(4-fluorophenyl)-1H-1,2,3-triazol-1-yl)ethyl)amino)-3-methylnaphthalene-1,4-dione (**11**)

Red solid; R_f 0.31 (hexane/ethyl acetate 1:1); IR (KBr, cm^{-1}): 3334, 3128, 2923, 1665, 1601, 1566, 1530, 1499, 1457; ^{1}H NMR (500 MHz, $CDCl_3$): δ 2.14 (3H, s), 4.13 (2H, t, *J* = 5.6 Hz), 4.63 (2H, t, *J* = 5.6 Hz), 5.59 (1H, bs), 7.08 (2H, t, *J* = 8.5 Hz), 7.58 (1H, t, *J* = 7.4 Hz), 7.66 (1H, t, *J* = 7.4 Hz), 7.72 (1H, s), 7.73-7.75 (2H, m), 7.97 (1H, d, *J* = 7.7 Hz), 8.03 (1H, d, *J* = 7.7 Hz); ^{13}C NMR (100 MHz, $CDCl_3$): 10.95, 45.05, 50.84, 115.42, 115.70, 115.92, 120.08, 126.02, 126.19,127.40, 127.48, 130.37, 132.18, 132.82, 134.28, 145.61, 147.22, 161.47, 163.93, 182.26, 183.32; HRMS (ESI): m/z calcd for $C_{21}H_{18}N_4O_2F$ $(M+H)^+$ 377.1408 found 377.1402.

2-((2-(4-(4-chlorophenyl)-1H-1,2,3-triazol-1-yl)ethyl)amino)-3-methylnaphthalene-1,4-dione (**12**)

Orange solid; R_f 0.32 (hexane/ethyl acetate 1:1); IR (KBr, cm^{-1}): 3217, 3126, 2923, 1678, 1607, 1568, 1520, 1480, 1462; ^{1}H NMR (500 MHz, $CDCl_3$): δ 2.15 (3H, s), 4.13 (2H, t, *J* = 5.4 Hz), 4.63 (2H, t, *J* = 5.4 Hz), 7.37 (2H, dt, *J* = 8.5, 1.9 Hz), 7.59 (1H, td, *J* = 7.6, 1.2 Hz), 7.67 (1H, td, *J* = 7.6, 1.2 Hz), 7.70 (2H, dt, *J* = 8.5, 1.9 Hz), 7.98 (1H, dd, *J* = 7.6, 1.0 Hz), 8.05 (1H, dd, *J* = 7.6, 1.0 Hz); ^{13}C NMR (100 MHz, $CDCl_3$): 10.96, 45.06, 50.90, 115.58, 120.36, 126.05, 126.24, 126.96, 128.67, 129.05, 130.39, 132.23, 132.84, 134.32, 145.61, 147.08, 182.30, 183.35; HRMS (ESI): m/z calcd for $C_{21}H_{18}N_4O_2Cl$ $(M+H)^+$ 393.1113 found 393.1124.

2-((2-(4-(4-bromophenyl)-1H-1,2,3-triazol-1-yl)ethyl)amino)-3-methylnaphthalene-1,4-dione (**13**)

Orange solid; R_f 0.32 (hexane/ethyl acetate 1:1); IR (KBr, cm^{-1}): 3223, 3124, 2923, 1675, 1606, 1568, 1518, 1462; ^1H NMR (400 MHz, $CDCl_3$): δ 2.15 (3H, s), 4.13 (2H, br), 4.63 (2H, t, *J* = 5.6 Hz), 5.56 (1H, bs), 7.52 (2H, dt, *J* = 8.5, 1.8 Hz), 7.58 (1H, td, *J* = 7.5, 1.3 Hz), 7.63-7.69 (3H, m), 7.75 (1H, s), 7.97 (1H, dd, *J* = 7.5, 1.2 Hz), 8.04 (1H, dd, *J* = 7.7, 1.2 Hz); ^{13}C NMR (100 MHz, $CDCl_3$): 10.97, 45.06, 50.91, 115.58, 120.39, 122.22, 126.04, 126.23, 127.22, 129.12, 130.39, 131.99, 132.23, 134.32, 145.60, 147.09, 182.30, 183.34; HRMS (ESI): m/z calcd for $C_{21}H_{17}N_4O_2BrNa$ $(M+Na)^+$ 459.0427 found 459.0424.

2-methyl-3-((2-(4-(pyridin-2-yl)-1H-1,2,3-triazol-1-yl)ethyl)amino)naphthalene-1,4-dione (**14**)

Orange solid; R_f 0.58 (chloroform/methanol 19:1); IR (KBr, cm^{-1}): 3256, 2924, 1669, 1605, 1571, 1518, 1466, 1418; ^1H NMR (400 MHz, $CDCl_3$): δ 2.15 (3H, s), 4.15 (2H, q, *J* = 5.9 Hz), 4.66 (2H, t, *J* = 5.9 Hz), 5.62 (1H, bs), 7.22 (1H, m), 7.61 (2H, m), 7.77 (1H, q), 7.95-8.05 (2H, m), 8.13-8.20 (2H, m), 8.54 (1H, br); ^{13}C NMR (125 MHz, $CDCl_3$): δ 10.88, 45.0, 50.84, 115.22, 120.27, 122.69, 122.97, 126.05, 126.12, 130.40, 132.11, 132.82, 134.18, 136.97, 145.63, 148.60, 149.27, 149.81, 182.16, 183.33; HRMS (ESI): m/z calcd for $C_{20}H_{18}N_5O_2$ $(M+H)^+$ 360.1455 found 360.1457.

2-methyl-3-((2-(4-(pyridin-3-yl)-1H-1,2,3-triazol-1-yl)ethyl)amino)naphthalene-1,4-dione (**15**)

Orange solid; R_f 0.33 (chloroform/methanol 19:1); IR (KBr, cm^{-1}): 3221, 3122, 2924, 1672, 1608, 1568, 1518, 1469; ^1H NMR (400 MHz, $CDCl_3$): δ 2.15 (3H, s), 4.15 (2H, q, *J* = 5.1 Hz), 4.67 (2H, t, *J* = 5.5 Hz), 5.62 (1H, br), 7.40 (1H, br), 7.59 (1H, td, *J* = 7.5, 1.3 Hz), 7.66 (1H, td, *J* = 7.5, 1.3 Hz), 7.87 (1H, s), 7.98 (1H, dd, *J* = 7.7, 1.1 Hz), 8.04 (1H, *J* = 7.7, 1.1 Hz), 8.22 (1H, d), 8.57 (1H, bs), 8.94 (1H, bs); ^{13}C NMR (125 MHz, $CDCl_3$): δ 11.00, 45.04, 51.00, 115.70, 120.72, 123.82, 126.08, 126.25, 130.38, 132.28, 133.18, 134.35, 146.85, 149.21; HRMS (ESI): m/z calcd for $C_{20}H_{18}N_5O_2$ $(M+H)^+$ 360.1455 found 360.1469.

2-((2-(4-benzyl-1H-1,2,3-triazol-1-yl)ethyl)amino)-3-methylnaphthalene-1,4-dione (**16**)

Red solid; R_f 0.51 (hexane/ethyl acetate 1:2.3); IR (KBr, cm^{-1}): 3331, 2923, 2853, 1660, 1631, 1601, 1569, 1521, 1463; ^1H NMR (500 MHz, $CDCl_3$): δ 2.09 (3H, s), 4.06 (4H, m), 4.50 (2H, t, *J* = 5.6 Hz), 5.54 (1H, bs), 7.15 (1H, s), 7.18-7.22 (3H, m), 7.25-7.28(2H, m), 7.60 (1H, td, *J* = 7.6, 1.3 Hz), 7.68 (1H, td, *J* = 7.6, 1.3 Hz), 7.98 (1H, dd, *J* = 7.6, 1.0 Hz), 8.07 (1H, dd, *J* = 7.6, 1.0 Hz); ^{13}C NMR (125 MHz, $CDCl_3$): δ 10.83, 32.12, 44.91, 50.48, 114.91, 122.15, 125.99, 126.13, 126.48, 128.57, 128.61, 130.36, 132.11,132.85, 134.22, 138.71, 145.53, 148.05, 182.09, 183.24; HRMS (ESI): m/z calcd for $C_{22}H_{21}N_4O_2$ $(M+H)^+$ 373.1659 found 373.1652.

dimethyl 1-(2-((3-methyl-1,4-dioxo-1,4-dihydronaphthalen-2-yl)amino)ethyl)-1H-1,2,3-triazole-4,5-dicarboxylate (**17**)

Red solid; R_f 0.33 (hexane/ethyl acetate 1:1); IR (KBr, cm^{-1}): 3324, 2923, 2853, 1734, 1666, 1618, 1594, 1566, 1517; ^1H NMR (400 MHz, $CDCl_3$): δ 2.11 (3H, s), 3.93 (3H, s), 3.95 (3H, s), 4.13 (2H, br), 4.89 (2H, t), 5.59 (1H, bs), 7.59 (1H, td, *J* = 7.5, 1.3 Hz), 7.68 (1H, td, *J* = 7.5, 1.3 Hz), 7.98 (1H, dd, *J* = 7.5, 0.9 Hz), 8.06 (1H, dd, *J* = 7.5, 0.9 Hz); ^{13}C NMR (125 MHz, $CDCl_3$): δ 10.69, 44.80, 50.46, 52.69, 53.49, 114.98, 125.95, 126.06, 130.09, 130.33, 132.10, 132.75, 134.15, 140.04, 145.50, 158.83, 160.16, 181.97, 183.24; HRMS (ESI): m/z calcd for $C_{19}H_{18}N_4O_6Na$ $(M+Na)^+$ 421.1119 found 421.1115.

diethyl 1-(2-((3-methyl-1,4-dioxo-1,4-dihydronaphthalen-2-yl)amino)ethyl)-1H-1,2,3-triazole-4,5-dicarboxylate (**18**)

Red solid; R_f 0.54 (hexane/ethyl acetate 1:1); IR (KBr, cm^{-1}): 3363, 3064, 2981, 2929, 1738, 1719, 1665, 1621, 1594, 1569; ^1H NMR (500 MHz, $CDCl_3$): δ 1.36 (3H, t, *J* = 7.1 Hz), 1.40 (3H, t, *J* = 7.1 Hz), 2.12 (3H, s), 4.13 (2H, t, *J* = 5.6 Hz), 4.39 (2H, q, *J* = 7.1 Hz), 4.42 (2H, q, *J* = 7.1 Hz), 4.88 (2H, t, *J* = 5.6 Hz), 5.62 (1H, bs), 7.59 (1H, td, *J* = 7.6, 1.2 Hz), 7.67 (1H, td, *J* = 7.6, 1.2 Hz), 7.98 (1H, d, *J* = 7.6 Hz), 8.06 (1H, d, *J* = 7.6 Hz); ^{13}C NMR (100 MHz, $CDCl_3$): δ 10.74, 13.75, 14.09, 44.85, 50.35, 61.92, 63.10, 114.96, 125.97, 126.09, 130.01, 130.35, 132.09, 132.80, 134.15, 140.46, 145.54, 158.47, 159.93, 181.98, 183.28; HRMS (ESI): m/z calcd for $C_{21}H_{23}N_4O_6$ $(M+H)^+$ 427.1612 found 427.1611.

Biology

Cytotoxicity screening using MTT assay

The cytotoxicity of the compounds was determined using MTT assay [16]. 1×10^4 cells/well were seeded in 100 μL DMEM, supplemented with 10% FBS in each well of 96-well microculture plates and incubated for 24 h at 37 ^oC in a CO_2 incubator. After 24 h of incubation all the synthesized compounds were added to the cells and incubated for 48 h. After 48 h of drug treatment, 10 μL MTT (3-(4, 5-dimethylthiazol-2-yl)- 2,5-diphenyl tetrazolium bromide) (5 mg/mL) was added to each well and the plates were further incubated for 4 h. Then the supernatant from each well was carefully removed, formazon crystals were dissolved in 100 μL of DMSO and absorbance at 570 nm wavelength was recorded.

Cell cycle analysis

Flow cytometric analysis (FACS) was performed to evaluate the distribution of the cells through the cell-cycle phases. MCF-7 cells were treated with compound **6** at 5, 7.5 and 10 μM concentrations for 48 h. Untreated and treated cells were harvested, washed with phosphate-buffered saline (PBS), fixed in ice-cold 70% ethanol, and stained with propidium iodide (Sigma–Aldrich). Cell cycle analysis was performed by flow cytometry (Becton Dickinson FACS Caliber instrument) [17].

Hoechst staining

MCF-7 cells were seeded at a density of 10,000 cells over 18 mm cover slips and incubated for 24 h. After incubation, cells were treated with the compound **6** at 5, 7.5

and 10 μM concentrations for 48 h. Hoechst 33258 (Sigma Aldrich) was added to the cells at a concentration of 0.5 mg/mL and incubated for 30 min at 37 °C. Later, the cells were washed with phosphate buffered saline (PBS). Cells from each cover slip were captured from randomly selected fields under fluorescent microscope (Olympus microscope) to qualitatively determine the proportion of viable and apoptotic cells based on their relative fluorescence and nuclear fragmentation [18].

Measurement of mitochondrial membrane potential (*$\Delta\Psi$m*)

MCF-7 (1×10^6 cells/well) cells were cultured in six-well plates. After plating, cells were treated with compound **6** at 5, 7.5 and 10 μM concentrations for 48 h. After 48 h of treatment, cells were collected by trypsinization and washed with PBS followed by resuspending in JC-1 (5,5,6,6-tetrachloro-1,1,3,3-tetraethylbenzimidazolocarbocyanine iodide-5μg/mL) and incubated at 37 ^{0}C for 15 min. Cells were rinsed three times with medium and suspended in pre warmed medium. The cells were then subjected to flow cytometric analysis on a flow cytometer (Becton Dickinson) in the FL1, FL2 channel to detect mitochondrial potential [19].

Annexin V-FITC assay for apoptosis

MCF-7 (1×10^6) cells were seeded in six-well plates and allowed to grow overnight. The medium was then replaced with complete medium containing compound **6** at 5, 7.5 and 10 μM concentrations for 48 h. After 48 h of drug treatment, cells from the supernatant and adherent monolayer cells were harvested by trypsinization, washed with PBS at 5000 rpm. Then the cells were stained with Annexin VFITC and propidium iodide using

the Annexin-V-FITC apoptosis detection kit (Sigma aldrich). Then the samples were analyzed by flow cytometry as described earlier [20].

Results and discussions

Chemistry

The target menadione-1,2,3-triazole hybrids (**4-18**) were synthesized in a three step protocol. As illustrated in **scheme 1**, initially azidoaminoalkanes (**2a-2d**) were prepared by literature procedures [21]. These compounds (**2a-2d**) upon treating with menadione (**1**) in DCM afforded Michael adducts (**3a-d)** in moderate yields. Addition of these azidoaminoalkanes to menadione was confirmed by ^{1}H NMR, ^{13}C NMR, mass and IR. In the ^{13}C NMR spectra, an upfield shift of C-2 carbon peak to δ 112-113 ppm indicated the attachment of azidoaminoalkane linker at C-3 position of menadione **1**. Further, in IR absorption signal in the range of 2093-2103 cm^{-1} indicated the presence of azido group for the compounds **3a-d**. Based on the higher cytotoxicity of **3a**, it was chosen as the key intermediate to synthesize the target hybrids by employing copper catalyzed azide-alkyne cycloaddition (CuAAC) with various alkynes. As shown in **scheme 2**, reactions of compound **3a** with alkynes in the presence of sodium ascorbate and $CuSO_4.5H_2O$ in THF/H_2O afforded the desired hybrid compounds (**4-18**) in good to excellent yield (**Table 1**). All the newly synthesized hybrid compounds were characterized by ^{1}H and ^{13}C NMR, IR and HRMS. As a representative case, ^{1}H NMR assignments of compound **6** was described in **Figure 2.** In the ^{1}H NMR spectra, the singlet of methine proton at δ 7.15-8.18 ppm indicated the triazole ring formation. The four protons of ethylene (-CH_2-CH_2-) linker connected to the triazole ring appeared in the region δ 4.05-4.89 ppm. The protons of -CH_3 group attached to quinone moiety

appeared at δ 2.09-2.15 ppm as singlet. In addition, the aromatic moiety protons and pyridyl group protons appeared in the region δ 6.93-8.94 ppm.

Biological evaluation

In vitro cytotoxicity

The *in vitro* cytotoxicity of synthesized compounds was carried out against a panel of five cancer cell lines, namely MCF-7 (breast), A549 (lung), Hela (cervical), DU-145 (prostate) and B-16 (mouse melanoma) by employing MTT assay [16]. Tamoxifen along with compound **1** were used as the reference standards in this study. The results are summarized in **Table 2** and expressed as IC_{50} values. It has been observed that compound **3a** showed significant activity when compared to remaining Michael adducts (**3b-3d)** against all the tested cell lines except Hela cell line. When the length of alkyl chain is increased from ethylene to pentyl, the activity decreased against most of the tested cell lines. It prompted us to choose the compound **3a** as the key intermediate to synthesize the target menadione based 1,2,3-triazole hybrids. From the IC_{50} values, it is evident that majority of synthesized hybrids displayed promising anticancer activity against the tested cell lines.

The efficacy order of the synthesized hybrids for each cell line is (IC_{50}):

A549: **9** (8.33 μM) > **6** (9.19 μM) > **5** (9.23 μM);

DU-145: **5** (7.81 μM) > **9** (7.95 μM) > **6** (8.02 μM) > **7** (8.84 μM) > **12** (9.35 μM) > **13** (9.56 μM);

Hela: **18** (10.36 μM) > **5** (10.72 μM);

MCF-7: **6** (8.73 μM) > **14** (10.48 μM);

B-16: **14** (9.23 μM) > **13** (12.59) > **5** (12.76 μM).

Among the synthesized hybrids, compound **5** displayed significant activity against all the cell lines (IC_{50} 7.81–12.76 μM). However, its activity was found to be maximum on DU-145 (IC_{50} 7.81 μM). Compound **6** exhibited significant activity against A549 (IC_{50} 9.19 μM), DU-145 (IC_{50} 8.02 μM) and MCF-7 (IC_{50} 8.73 μM) cell lines and compound **7** exhibited significant activity against DU-145 (IC_{50} 8.84 μM). The presence of halogens on **11, 12** and **13** increased activity significantly against all the cell lines. In particular, compounds **12** (IC_{50} 9.35–14.99 μM) and **13** (IC_{50} 9.56–13.18 μM) containing chlorine and bromine atoms respectively exhibited potent activity against all the cell lines. Surprisingly, compound **4** with an unsubstituted phenyl moiety exhibited weak cytotoxicity against almost all the cell lines tested. Hence, the substitution on the phenyl ring either with an alkyl group or halo group is important for better anticancer activity. The replacement of phenyl group of compound **4** by a pyridyl group (**14** and **15**) resulted in increase of activity against all the tested cell lines. The triazole hybrid **18** formed by diethyl acetylenedicarboxylate showed better activity than dimethyl acetylenedicarboxylate hybrid **17**. Specifically, compound **6** showed significant activity against human breast cancer cell line (MCF-7) with IC_{50} value of 8.73 μM whereas the parent compound menadione **1** showed 13.87 μM against the MCF-7. Based on the promising anticancer activity, compound **6** was taken up for further mechanism of cell growth inhibition studies.

Cell cycle analysis

Many anticancer compounds exert their growth inhibitory effect either by arresting the cell cycle at a particular checkpoint of cell cycle or by induction of apoptosis or a combined effect of both cycle block and apoptosis [22, 23]. The *in vitro* screening

results revealed that compound **6** showed significant activity against human breast cancer cell line, MCF-7. Therefore, it was considered of interest to understand whether this inhibition of cell growth was on account of cell cycle arrest. In this study MCF-7 cells were treated with this compound at concentrations of 5, 7.5 and 10 μM for 48 h. Results indicated that this compound arrested the cell cycle at G0/G1 phase and suggesting that this compound **6** interferes with breast cancer cell proliferation by arresting the cell cycle at G0/G1 phase of cell cycle (**Figure 3** and **Table 3**).

Morphological analysis for apoptosis with Hoechst staining

Apoptosis is one of the main pathways that lead to cell death in which the chromatin condensation and fragmented nuclei are known as the classic characteristics [18]. In this context, it was considered of interest to investigate the apoptotic inducing effect of the potent compound (**6**) by Hoechst staining (H 33258) method in MCF-7 breast cancer cell line. In this study, MCF-7 cells were treated with compound **6** at 5, 7.5 and 10 μM concentrations for 48 h. This compound showed significant effect on the nuclear condensation in comparison to the untreated control cells as shown in **Figure 4.** These results demonstrated that this compound is effective in inducing cellular apoptosis.

***Measurement of mitochondrial membrane potential* (ΔΨm)**

The maintenance of mitochondrial membrane potential (ΔΨm) is significant for mitochondrial integrity and bio energetic function [24]. Mitochondrial changes, including loss of mitochondrial membrane potential (ΔΨm), are the key events that take place during drug-induced apoptosis. Mitochondrial injury by compound **6** was evaluated by detecting drop in mitochondrial membrane potential (ΔΨm). In this study, we have

investigated the involvement of mitochondria in the induction of apoptosis by compound **6**. After 48 h of drug treatment with this compound at 5, 7.5 and 10 μM concentrations, a reduction in mitochondrial membrane potential ($\Delta\Psi m$) was observed in MCF-7 cells, as assessed by JC-1 staining (**Figure 5**).

Annexin V-FITC for apoptosis

The apoptotic effect of compound **6** was further evaluated by Annexin V FITC/PI (AV/PI) dual staining assay [25] to examine the occurrence of phosphatidylserine externalization and also to understand whether it is due to physiological apoptosis or nonspecific necrosis. In this study MCF-7 cells were treated with compound **6** for 48 h at 5, 7.5 and 10 μM concentrations to examine the apoptotic effect. It was observed that this compound showed significant apoptosis against MCF-7 cells as shown in **Figure 6**.

Conclusion

In conclusion, fifteen novel menadione-1,2,3-triazoles have been synthesized by employing three step protocol and evaluated for their anticancer activity against five cancer lines. The results of *in vitro* cytotoxicity indicated that hybrid compounds **5, 6** and **9** were more potent than the standard tamoxifen against A549 cell line. Compounds **5**, **6**, **7**, **9**, **12**, **13** were more potent than the standard tamoxifen against DU-145 cell line. Compounds **5, 12, 13** and **18** were more potent than the standard tamoxifen against Hela cell line. Compound **6** was more potent than the standard tamoxifen and parent menadione against MCF-7 cell line. The in depth biological studies showed that the anticancer activity of hybrid compound **6** could be attributed to the induction of cell cycle arrest and apoptosis in human breast (MCF-7) cancer cell line.

Acknowledgements

We are thankful to Director, CSIR- IICT for support and encouragement. CVP is grateful to CSIR, New Delhi, India for providing fellowship.

Conflict of Interest

The authors declare that there is no conflict of interest.

Legends

Figure 1. Examples of quinones and 1,2,3-triazoles that are in clinical use or trials

Figure 2. ^{1}H NMR assignments of compound **6**

Figure 3. Flow cytometric analysis in MCF-7 breast cancer cell line after treatment with compound **6**

Figure 4. Hoechst staining in MCF-7 cell line

Figure 5. Drops in membrane potential ($\Delta\Psi$m) were assessed by JC-1 staining of MCF-7 cells treated with compound **6**

Figure 6. Annexin V-FITC staining

Scheme 1. Synthesis of compounds 3a-d

Scheme 2. Synthesis of compounds 4-18

Table 1. Menadione-1,2,3- triazole hybrids (4-18)

Table 2. IC_{50} (in μM) values for the synthesized compounds on selected cancer cell lines

Table 3. Cell cycle analysis in breast cancer cell line, MCF-7

References

1. Kumagai Y, Shinkai Y, Miura T, Cho AK (2012) The chemical biology of naphthoquinones and its environmental implications. Annu Rev Pharmacol Toxicol 52:221–247. doi: 10.1146/annurev-pharmtox-010611-134517

2. El-Najjar N, Gali-Muhtasib H, Ketola RA, et al (2011) The chemical and biological

activities of quinones: Overview and implications in analytical detection. Phytochem Rev 10:353–370. doi: 10.1007/s11101-011-9209-1

3. Wellington KW (2015) Understanding cancer and the anticancer activities of naphthoquinones – a review. RSC Adv 5:20309–20338. doi: 10.1039/C4RA13547D

4. Mallavadhani UV, Prasad CV, Shrivastava S, Naidu VGM (2014) Synthesis and anticancer activity of some novel 5,6-fused hybrids of juglone based 1,4-naphthoquinones. Eur J Med Chem 84–91. doi: 10.1016/j.ejmech.2014.06.012

5. Lamson DW, Plaza SM (2003) The anticancer effects of vitamin K. Altern Med Rev 8:303–318.

6. Lu J-J, Bao J-L, Wu G-S, et al (2013) Quinones derived from plant secondary metabolites as anti-cancer agents. Anticancer Agents Med Chem 13:456–63. doi: 10.2174/187152013804910389

7. Wu FYH, Sun TP (1999) Vitamin K3 induces cell cycle arrest and cell death by inhibiting Cdc25 phosphatase. Eur J Cancer 35:1388–1393. doi: 10.1016/S0959-8049(99)00156-2

8. Nutter LM, Ann-Lii C, Hsiao-Ling H, et al (1991) Menadione: Spectrum of anticancer activity and effects on nucleotide metabolism in human neoplastic cell lines. Biochem Pharmacol 41:1283–1292. doi: 10.1016/0006-2952(91)90099-Q

9. Nakaoka ERI, Tanaka S, Onda K, et al (2015) Effects of vitamin K 3 and K 5 on daunorubicin-resistant human T lymphoblastoid leukemia cells. Anticancer Res 35:6041–6048.

10. Shukla S, Wu C-P, Nandigama K, Ambudkar S V (2007) The naphthoquinones, vitamin K3 and its structural analogue plumbagin, are substrates of the multidrug resistance linked ATP binding cassette drug transporter ABCG2. Mol Cancer Ther 6:3279–3286. doi: 10.1158/1535-7163.MCT-07-0564

11. Adnan H, Antenos M, Kirby GM (2012) The effect of menadione on glutathione S-transferase A1 (GSTA1): C-Jun N-terminal kinase (JNK) complex dissociation in human colonic adenocarcinoma Caco-2 cells. Toxicol Lett 214:53–62. doi: 10.1016/j.toxlet.2012.08.007

12. He T, Hatem E, Vernis L, et al (2015) PRX1 knockdown potentiates vitamin K3 toxicity in cancer cells: a potential new therapeutic perspective for an old drug. J Exp Clin Cancer Res 34:152. doi: 10.1186/s13046-015-0270-2

13. González-Calderón D, Mejía-Dionicio MG, Morales-Reza MA, et al (2016) Azide-enolate 1,3-dipolar cycloaddition in the synthesis of novel triazole-based miconazole analogues as promising antifungal agents. Eur J Med Chem 112:60–65. doi: 10.1016/j.ejmech.2016.02.013

14. Dehaen W, Bakulev VA (2015) Chemistry of 1,2,3-triazoles. Springer,

International Publishing AG. doi: 10.1007/7081_2014_131

15. Agalave SG, Maujan SR, Pore VS (2011) Click chemistry: 1,2,3-triazoles as pharmacophores. Chem - An Asian J 6:2696–2718. doi: 10.1002/asia.201100432

16. Botta M, Armaroli S, Castagnolo D, et al (2007) Synthesis and biological evaluation of new taxoids derived from 2-deacetoxytaxinine J. Bioorg Med Chem Lett 17:1579–1583. doi: 10.1016/j.bmcl.2006.12.101

17. Szumilak M, Szulawska-Mroczek A, Koprowska K, et al (2010) Synthesis and in vitro biological evaluation of new polyamine conjugates as potential anticancer drugs. Eur J Med Chem 45:5744–5751. doi: 10.1016/j.ejmech.2010.09.032

18. Shankar R, Chakravarti B, Singh US, et al (2009) Synthesis and biological evaluation of 3,4,6-triaryl-2-pyranones as a potential new class of anti-breast cancer agents. Bioorg Med Chem 17:3847–3856. doi: 10.1016/j.bmc.2009.04.032

19. Chakravarti B, Maurya R, Siddiqui JA, et al (2012) In vitro anti-breast cancer activity of ethanolic extract of Wrightia tomentosa: Role of pro-apoptotic effects of oleanolic acid and urosolic acid. J Ethnopharmacol 142:72–79. doi: 10.1016/j.jep.2012.04.015

20. Browne LJ, Gude C, Rodriguez H, et al (1991) Fadrozole hydrochloride: a potent, selective, nonsteroidal inhibitor of aromatase for the treatment of estrogen-dependent disease. J Med Chem 34:725–736. doi: 10.1021/jm00106a038

21. Srinivasan R, Tan P, Wu H, et al (2009) High-throughput synthesis of azide libraries suitable for direct “ click ” chemistry and in situ screening. Org Biomol Chem 7:1821–1828. doi: 10.1039/b902338k

22. Chan KT, Meng FY, Li Q, et al (2010) Cucurbitacin B induces apoptosis and S phase cell cycle arrest in BEL-7402 human hepatocellular carcinoma cells and is effective via oral administration. Cancer Lett 294:118–124. doi: 10.1016/j.canlet.2010.01.029

23. Shen JK, Du HP, Yang M, et al (2009) Casticin induces leukemic cell death through apoptosis and mitotic catastrophe. Ann Hematol 88:743–752. doi: 10.1007/s00277-008-0677-3

24. Gonda K, Tsuchiya H, Sakabe T, et al (2008) Synthetic retinoid CD437 induces mitochondria-mediated apoptosis in hepatocellular carcinoma cells. Biochem Biophys Res Commun 370:629–633. doi: 10.1016/j.bbrc.2008.04.008

25. Zhu H, Zhang J, Xue N, et al (2010) Novel combretastatin A-4 derivative XN0502 induces cell cycle arrest and apoptosis in A549 cells. Invest New Drugs 28:493–501. doi: 10.1007/s10637-010-9424-4

Scheme 1

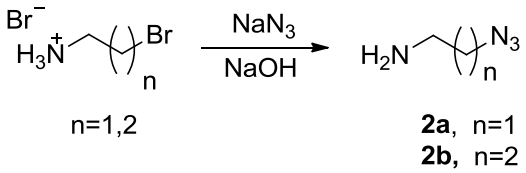

n=1,2

2a, n=1
2b, n=2

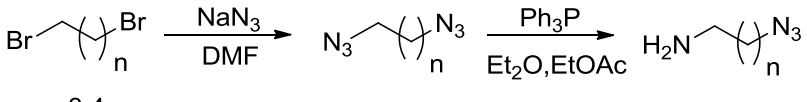

n=3,4

2c, n=3
2d, n=4

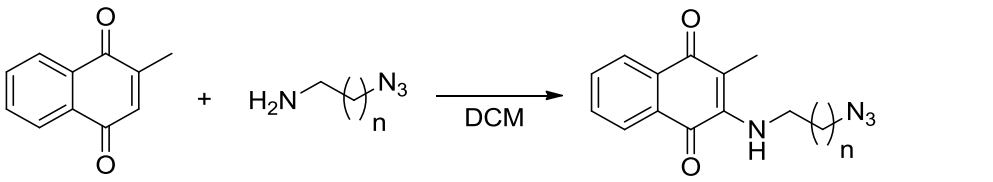

1 **2a-d** **3a-d** n=1,2,3,4

Scheme 2

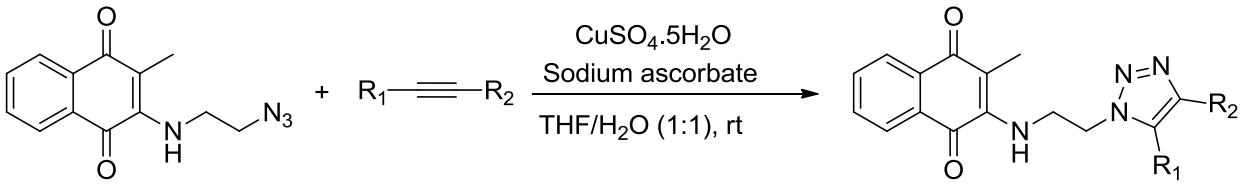

3a **4-18**

Table 1

Entry	Alkyne	Product	Yield (%)	mp (°C)
i	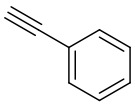	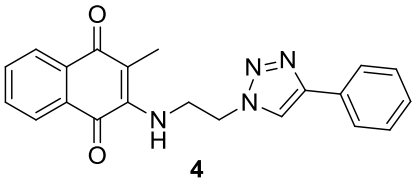 **4**	87	159-161
ii	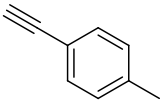	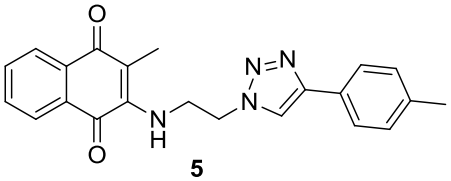 **5**	76	161-163
iii	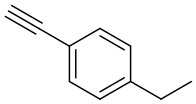	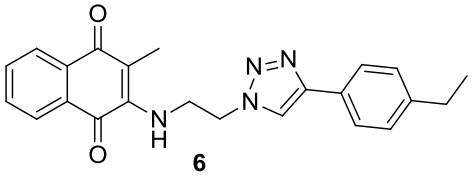 **6**	86	171-173
iv	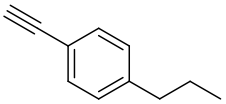	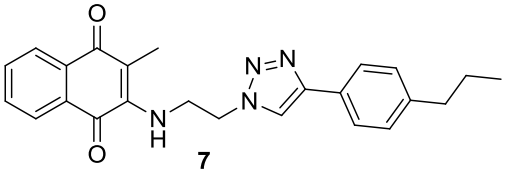 **7**	84	161-163
v	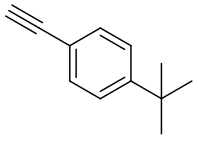	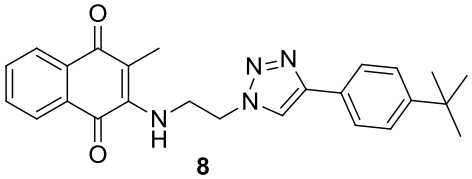 **8**	81	217-219
vi	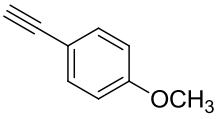	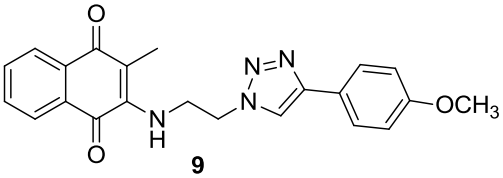 **9**	78	146-148
vii	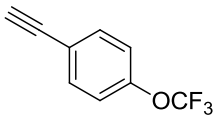	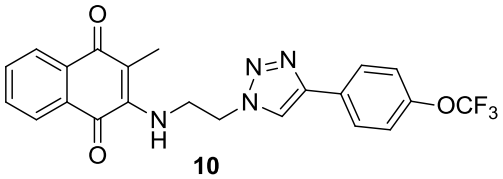 **10**	58	158-160
viii	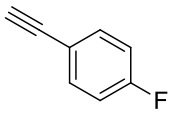	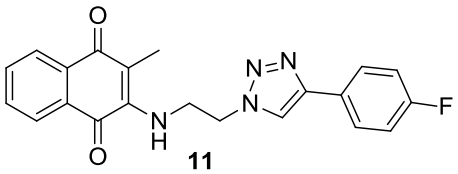 **11**	89	175-177

(continued on next page)

Table 1 *(continued)*

Entry	Alkyne	Product	Yield (%)	mp (°C)
ix	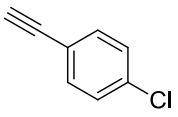	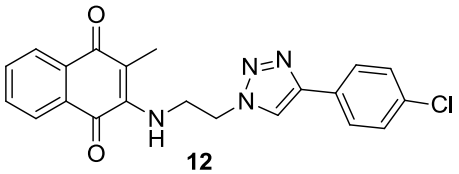 **12**	88	195-197
x	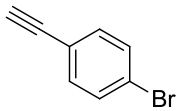	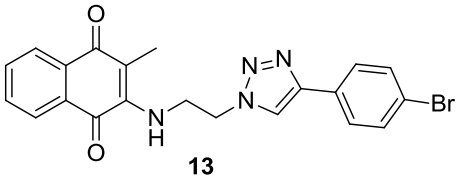 **13**	88	192-194
xi	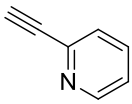	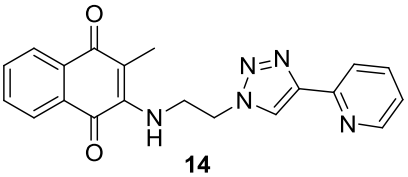 **14**	49	121-123
xii	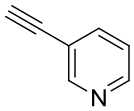	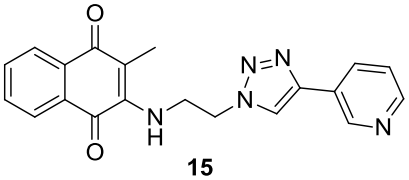 **15**	48	193-195
xiii	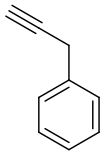	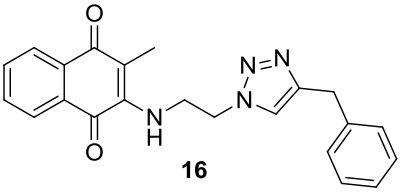 **16**	76	129-131
xiv	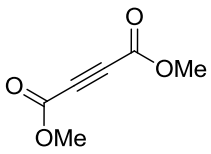	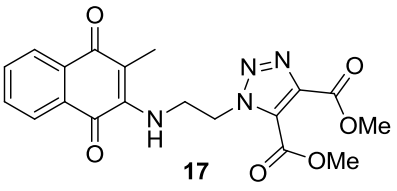 **17**	71	138-140
xv	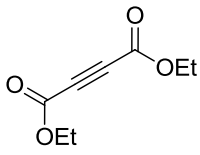	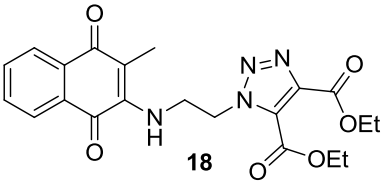 **18**	91	120-122

Table 2: IC_{50} values[a] (in μM) for the synthesized compounds on selected cancer cell lines

Compound	A549[b]	DU-145[c]	Hela[d]	MCF-7[e]	B-16[f]
1	6.14±0.04	4.32±0.07	8.45±0.19	13.87±3.01	8.92±0.65
3a	9.67±0.47	9.01±1.51	81.30±2.64	14.33±0.18	7.63±0.50
3b	9.69±0.14	7.50±0.06	14.68±0.14	21.59±1.47	15.66±0.31
3c	61.67±2.01	26.18±2.51	49.03±1.93	78.53±1.28	90.16±1.47
3d	109.68±3.57	23.69±0.72	76.86±0.81	26.36±0.57	27.40±0.70
4	67.78±4.26	18.62±0.61	121.64±5.88	60.78±0.31	54.16±7.94
5	**9.23±0.15**	**7.81±1.37**	**10.72±0.35**	12.67±0.13	12.76±0.64
6	**9.19±0.24**	**8.02±1.56**	26.16±2.85	**8.73**±0.85	20.19±0.99
7	**10.24±0.33**	**8.84**±1.00	30.72±3.64	39.23±6.51	27.46±2.91
8	17.32±2.21	12.40±0.06	20.15±0.08	13.67±0.70	14.85±0.37
9	**8.33**±0.54	**7.95**±0.26	20.31±0.02	27.84±2.17	13.67±1.11
10	37.24±3.63	31.21±5.44	51.43±8.50	76.50±0.51	ND
11	31.26±0.51	19.37±2.83	30.37±3.91	26.06±0.88	116.21±567
12	14.12±0.87	**9.35**±0.91	14.99±0.28	12.11±0.04	13.80±0.45
13	11.46±1.06	**9.56**±0.62	**13.18**±0.42	13.15±0.38	12.59±0.41
14	11.35±0.18	12.44±0.20	24.56±0.78	**10.48±0.68**	**9.23±0.15**
15	17.06±0.86	14.97±0.73	35.16±0.98	15.66±1.71	23.58±0.32
16	84.14±1.37	13.96±0.23	30.77±3.53	32.92±7.89	20.18±0.33
17	19.36±1.04	20.56±0.66	26.72±2.99	22.0±1.74	130.85±7.01
18	12.63±0.74	12.20±2.11	**10.36**±0.22	11.39±0.61	37.04±3.92
Tamoxifen	10.87±1.86	12.75±1.03	18.63±1.17	10.99±0.74	ND

Bold values indicate potent compounds. ND-Not determined

[a] 50% Inhibitory concentration after 48 h of drug treatment and the values are average of three individual experiments, [b] Human lung cancer, [c] Human prostate cancer, [d] Human cervical cancer, [e] Human breast cancer, [f] Mouse melanoma

Table 3: Cell cycle analysis in breast cancer cell line, MCF-7

Sample	Sub G1 %	G0/G1 %	S %	G2/M %
A: Control (MCF-7)	0.68	79.94	2.39	16.29
B: Compound **6** (5 μM)	0.55	84.55	1.61	12.80
C: Compound **6** (7.5 μM)	0.64	89.22	1.89	7.80
D: Compound **6** (10 μM)	0.71	96.99	1.04	0.78

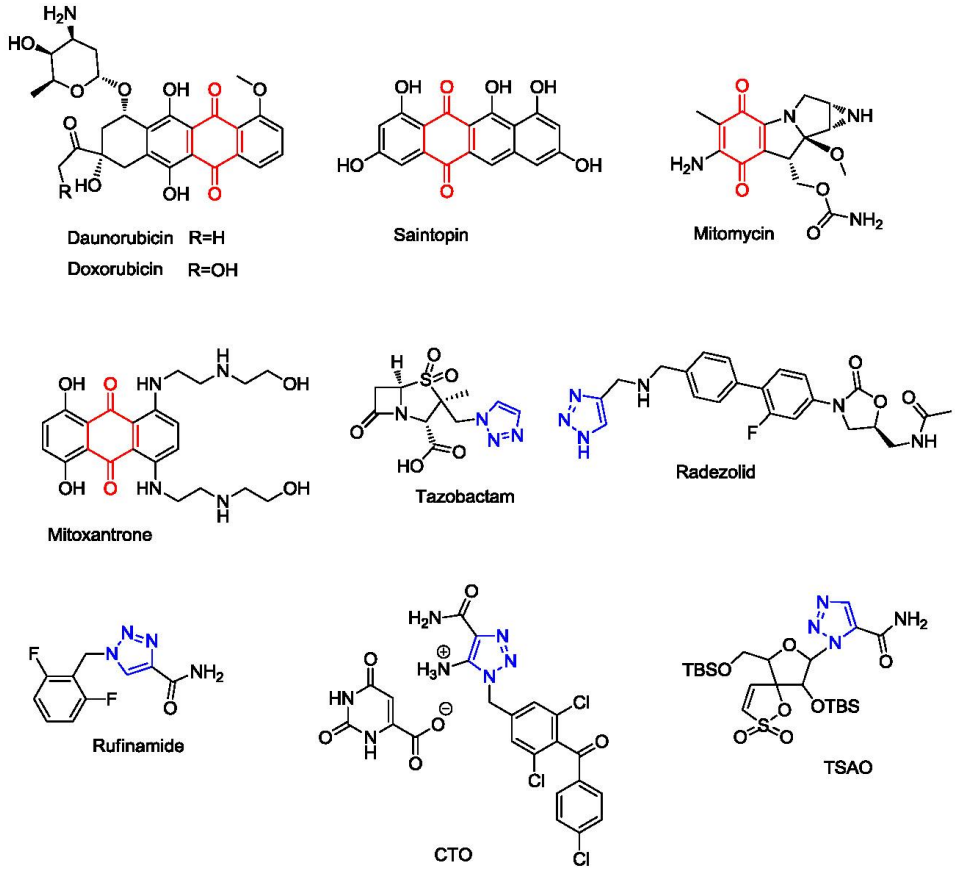

Figure 1. Examples of quinones and 1,2,3-triazoles that are in clinical use or trials

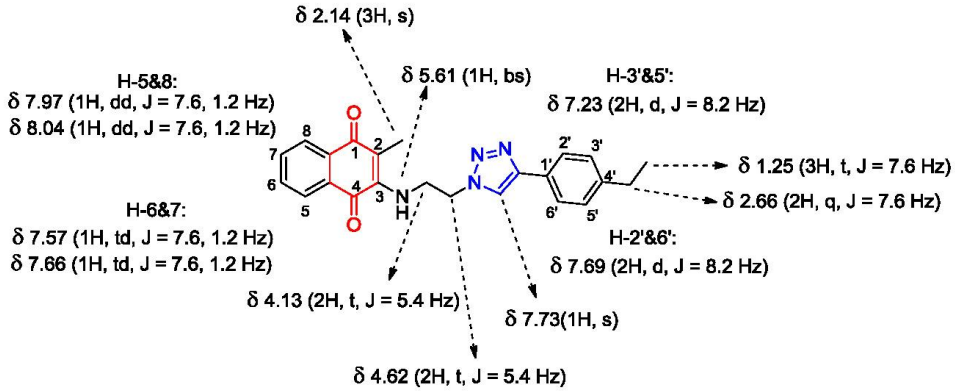

Figure 2. ^{1}H NMR assignments of compound **6**

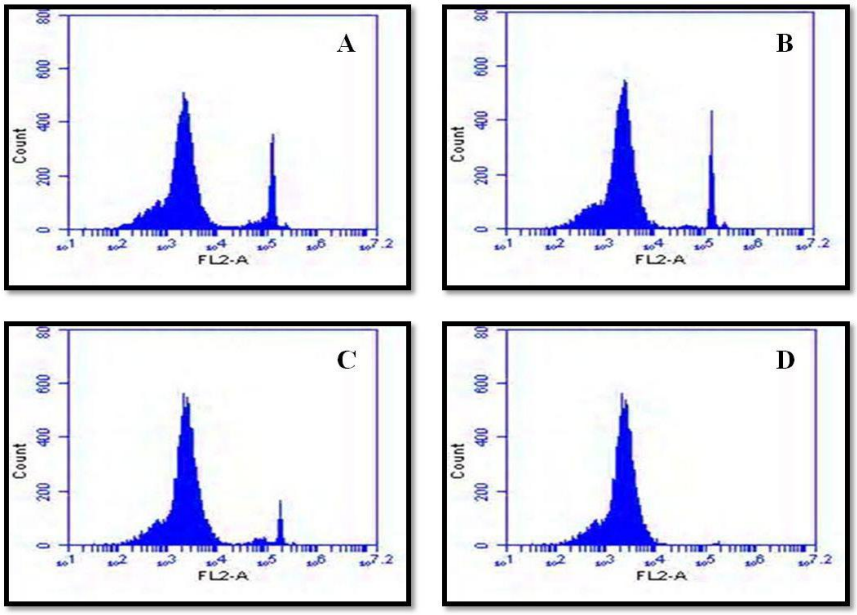

Figure 3. Flow cytometric analysis in MCF-7 breast cancer cell line after treatment with compound **6**. A: Untreated control cells (MCF-7), B: compound **6** (5 μM), C: compound **6** (7.5 μM) and D: compound **6** (10 μM).

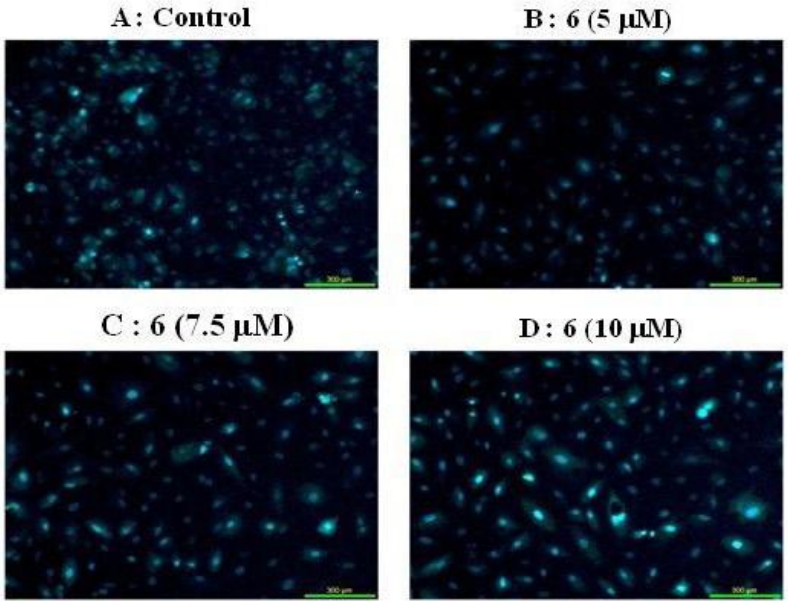

Figure 4. Hoechst staining in MCF-7 cell line; A: Control cells, B: compound 6 (5 μM), C: compound 6 (7.5 μM) and D: compound 6 (10 μM).

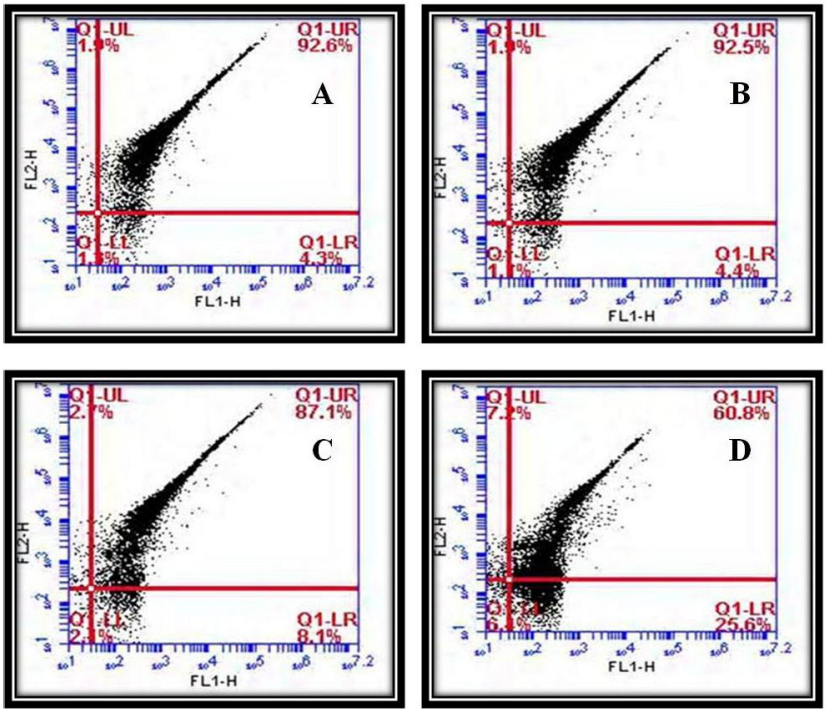

Figure 5. Drops in membrane potential ($\Delta\Psi$m) were assessed by JC-1 staining of MCF-7 cells treated with compound **6** and samples were then subjected to flow cytometry analysis on a FACScan (Becton Dickinson). A: Untreated control cells (MCF-7), B: compound **6** (5 μM), C: compound **6** (7.5 μM) and D: compound **6** (10 μM).

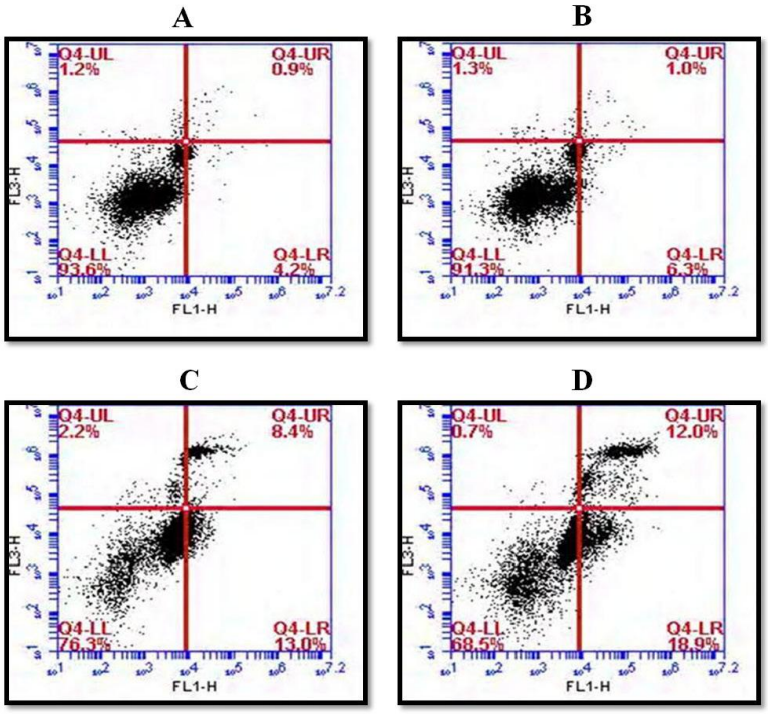

Sample	UL %	UR %	LL%	LR %
A: Control **(MCF-7)**	1.24	0.87	93.64	4.24
B: Compound 6 **(5 μM)**	1.35	1.04	91.31	6.30
C: Compound 6 **(7.5 μM)**	2.19	8.44	76.32	13.04
D: Compound 6 **(10 μM)**	0.65	12.04	68.45	18.85

Figure 6. Annexin V-FITC staining. A: Untreated control cells (MCF-7), B: compound **6** (5 μM), C: compound **6** (7.5 μM) and D: compound **6** (10 μM).